Submitted to International Journal of Solids and Structures

Multi-objective optimization for prestress design of cable-strut structures

Qing Ma[a, b], Makoto Ohsaki[b], Zhihua Chen[a,*], Xiangyu Yan[a, c]

[a] Department of Civil Engineering, Tianjin University, Tianjin, China

[b] Department of Architecture and Architectural Engineering, Kyoto University, Kyoto, Japan

[c] Architectural Design and Research Institute, Tianjin University, Tianjin, China

Abstract

Load bearing capacity of a cable-strut structure is dependent on the level and distribution of prestress. Although a higher prestress level enhances overall stiffness of the structure, this condition may demand larger member sectional areas and material cost. The effect of fabrication and installation error should also be incorporated in the prestress design. This paper presents a new optimization method for prestress design of cable-strut structures. A multi-objective optimization problem is formulated and solved to obtain preferred coefficient vectors of prestress modes with the following four objective functions: (1) minimize average area of members; (2) maximize minimum eigenvalue of stiffness matrix; (3) minimize prestress variance of cables; and (4) minimize maximum eigenvalue of error sensitivity matrix. Pareto optimal solutions are obtained by NSGA-II. Among the Pareto optimal solutions, the most preferred solution is selected using PROMETHEE-II. Two examples are presented to illustrate the proposed process. The results are compared with those by existing methods of optimization with a single objective function. Significance of each objective function is also evaluated by the number of remaining Pareto optimal solutions after removal of the objective function.

Keywords

cable-strut structures, cable dome, prestress design, multi-objective optimization

1 Introduction

Based on the concept of isolated compression among continuous tension, Snelson (1996) proposed the concept of tensegrity structure, which was named by Fuller (1975). From the 1950s to the 1980s, a series of tensegrity sculptures were made by Fuller (1975), Snelson (1996) and Emmerich (1996), etc. Researchers and engineers then utilized the high structural efficiency of the tensegrity structure into the design of long-span structures. Tensegrity grid was proposed by Motro (2003). Cable dome structure was invented by Geiger (1986) and first applied in the design of Seoul Olympic Gymnastics Arena. Cable dome was then modified by Levy (1994) with triangular units to design the Georgia Dome. Cable truss structures were also used in canopies of large stadiums. These structures consisting of cables and struts are in general called *cable-strut structures*.

Since a cable-strut structure is stiffened by applying prestress to the members, its load bearing capacity depends on the prestress level and distribution . There are two processes of obtaining feasible prestress conforming to the unilateral conditions of stresses in cables and struts: (1) form finding process to modify the geometry and prestress simultaneously; (2) prestress design to obtain optimal prestresses under given geometry. We focus on the process of prestress design in this paper.

Various studies have been conducted to find the optimal prestress of cable-strut structures. Kiewitt cable dome was optimized by minimizing the prestress of the outmost hoop (Yuan *et al*., 2007) and minimizing its total strain energy (Chen *et al.*, 2015). The first natural frequency of the tensegrity grid was maximized to achieve larger structural stiffness (Safeai *et al*., 2012; Lee and Lee, 2014). Moreover, the minimum eigenvalue of tangent stiffness matrix was maximized for the form finding of tensegrity structures using ant colony systems (Chen *et al*., 2012). The first natural frequency and frequency gap between the first two modes were maximized for the assembly of modular tensegrity structures (Ashwear *et al*., 2016). Zhang and Feng (2017) obtained the optimum prestress of cable-strut structures by maximizing the minimum eigenvalue of geometric stiffness matrix with the constraints on prestress variance and structural stability. In the prestress design process of cable-strut structures, various requirements are to be considered for member stress, overall stiffness, slenderness of members, etc. Although the cable-strut structures are stiffened by the prestresses that are in self-equilibrium state, their values should be at an appropriate level. A relatively high level of prestress may demand larger material cost, and it may also induce stiffness degradation in cable-strut structures (Chen *et al*, 2018a). Therefore, appropriate prestress values of prestress should be determined in view of compromise among several design requirements. Accordingly, the optimization problem for prestress design should be formulated as a multi-objective optimization problem to find a set of compromise solutions called Pareto optimal solutions(referred to as Pareto solutions for brevity)..

Multi-objective optimization has been extensively studied in the field of operations research and structural optimization. It is regarded that the process of multi-objective optimization is basically interactive, and the best solution is to be found based on the additional preference function (Branke et al, 2008). This process is called Multiple Criteria Decision Analysis (MCDA) (Figueira et al, 2005). Among various approaches of MCDA such as ELECTRE method and UTA method, we use the PROMETHEE-II method (Preference Ranking Organization METHod for Enrichment Evaluations) (Brans *et al*, 1986) that is categorized as an outranking method.

It should be noted that most of the studies of multi-objective optimization in prestress design of cable-strut structures consider only two objective functions. It is rather easy to investigate properties of two-objective Pareto solutions mathematically or visually. However, visualization becomes very difficult for Pareto solutions with more than three functions (Tušar and Filipič, 2015; Brockoff *et al*., 2008). Furthermore, redundant objective functions should be removed to enhance convergence of optimization process and efficiency in presenting solutions. It is easy to detect redundant objective functions for a linear problem (Gal and Leberling, 1977). For a nonlinear problem, principal component analysis and conflict-based approaches have been proposed (Brockoff *et al*., 2008).

For tensegrity structures, there are some studies of prestress design considering two objective functions. The tensegrity grid was optimized for maximizing the minimum eigenvalue of the tangential stiffness matrix and minimizing compliance as a measure of flexibility (Ohsaki *et al*., 2008), and maximizing the minimum eigenvalue of the tangential stiffness matrix and minimizing prestress deviation (Ohsaki *et al*., 2012). Multi-objective optimization is also applied in other areas of application of tensegrity structures. Xu and Luo (2008) optimized the active tensegrity structures by minimizing the distance between real and design shapes and the length change of adjustable members. Adam and Smith (2007) obtained the control scheme for active tensegrity considering four objectives: maintaining the slope of the top surface, maintaining the actuator jacks at its midpoint, minimizing the stress of members and maximizing the structural stiffness. However, previous studies of multi-objective optimization with only two objective functions are not comprehensively enough to cover the major influential factors in design process of cable-strut structures.

In this paper, four objective functions are taken into account. Pareto optimal solutions are obtained by Improved Non-dominated Sorting Genetic Algorithm (NSGA-II) (Deb *et al*., 2002). Among the Pareto optimal solutions, the most preferred solution is selected using PROMETHEE-II.

2 Optimization Problem

2.1 Variables and equilibrium equations

The prestress of structures with multiple self-stress modes is expressed as a linear combination of self-stress modes. In practical design, the level and distribution of prestress are decided with respect to various structural and architectural demands. Therefore, the process of prestress design becomes a problem of obtaining the optimum combination of self-stress modes in order to meet multiple design requirements. Derivation of equilibrium equation is briefly explained below. See, e.g. Pellegrino and Calladine (1986) and Zhang and Ohsaki (2015) for details.

Connectivity of the nodes and members of the structure is defined by the connectivity matrix $\boldsymbol{C}$ (Schek, 1974). The vectors of coordinate differences in *x*-, *y*- and *z*-directions of the two end nodes of members are denoted by δ_x, δ_y and δ_z, respectively. Then the coordinate difference matrices Δ_x, Δ_y and Δ_z are defined as $\Delta_x = \mathrm{diag}(\delta_x)$, $\Delta_y = \mathrm{diag}(\delta_y)$ and $\Delta_z = \mathrm{diag}(\delta_z)$. The diagonal matrix consisting of member lengths is denoted as $\boldsymbol{L}$. Then the equilibrium matrix $\boldsymbol{D}^0$ including the support degrees of freedom is obtained as

$$\boldsymbol{D}^0 = \begin{bmatrix} \boldsymbol{C}^T \Delta_x \boldsymbol{L}^{-1} \\ \boldsymbol{C}^T \Delta_y \boldsymbol{L}^{-1} \\ \boldsymbol{C}^T \Delta_z \boldsymbol{L}^{-1} \end{bmatrix} \tag{1}$$

Equilibrium matrix $\boldsymbol{D}^0$ is reduced to $\boldsymbol{D}$ after removing the rows corresponding to the fixed displacement components.

For a cable-strut structure with s self-stress modes, its prestress vector $\boldsymbol{T}$ is expressed by the combination of self-stress modes as:

$$\boldsymbol{T} = \sum_{i=1}^{s} \alpha^i \boldsymbol{t}^i \tag{2}$$

where α^i is the combination coefficient corresponding to the ith self-stress vector $\boldsymbol{t}^i$ satisfying

$$\boldsymbol{D}\boldsymbol{t}^i = \boldsymbol{0} \tag{3}$$

The self-stress modes can be calculated by SVD of the equilibrium matrix $\boldsymbol{D}$ (Pellegrino and Calladine, 1986) if the geometry of the structure is given. Therefore, the combination coefficients $\boldsymbol{\alpha}$ are chosen to be the variables of optimization of prestress.

2.2 Objective functions

Construction of high strength/stiffness structures with less material is always the goal of structural engineers. The load bearing capacity of cable-strut structures are dependent on the prestresses applied to the members. However, larger prestress usually demands larger sectional area of members. Therefore, tangent stiffness is to be maximized while the material cost is to be minimized. Moreover, it is desirable that the values of prestress are almost uniform in cables, so that the member sizes of cables are almost uniform when the stresses have almost the same absolute values considering safety factor from the upperbound stress. In this section, four objective functions are defined for formulating a multi-objective programming problem.

2.2.1 Average area of members

Average area of members is equivalent to the sum of material volume if the topology and geometry of the structure are given. At the same time, the average area represents the approximate size of members, which is more intuitive for designers. Let L^i and A^i denote the area and length of member *i*, respectively. The average area A_{ave} of members can be calculated as

$$A_{\mathrm{ave}} = \frac{\sum_{i=1}^{n_m} L^i A^i}{\sum_{i=1}^{n_m} L^i} \tag{4}$$

where n_m is the number of members.

Let $T^i(\boldsymbol{\alpha})$ denote the prestress of member *i*, which is a function of $\boldsymbol{\alpha}$. The allowable stresses of material of cable and strut are denoted by σ_c (>0) and σ_s (<0), respectively. The cross-sectional area can be decided by

$$A^i(\boldsymbol{\alpha}) = \frac{T^i(\boldsymbol{\alpha})}{\eta\sigma_c} \quad \text{for cable} \tag{5}$$

$$A^i(\boldsymbol{\alpha}) = \frac{T^i(\boldsymbol{\alpha})}{\eta\varphi\sigma_s} \quad \text{for strut} \tag{6}$$

where η is the strength reduction coefficient considering uncertainty of loads, and the strength reduction coefficient φ considering buckling is also included for struts. Then, the first objective function $F_1(\boldsymbol{\alpha})$ is expressed as

$$F_1(\boldsymbol{\alpha}) = A_{\text{ave}}(\boldsymbol{\alpha}) \tag{7}$$

2.2.2 Minimum eigenvalue of stiffness matrix

The tangent stiffness matrix $\boldsymbol{K}_T$ of cable-strut structure is expressed as follows as the sum of the geometric stiffness matrix $\boldsymbol{K}_G$ due to the prestress and the linear stiffness matrix $\boldsymbol{K}_E$ composed of the axial stiffness of members:

$$\boldsymbol{K}_T = \boldsymbol{K}_E + \boldsymbol{K}_G \tag{8}$$

The linear stiffness matrix can be derived from

$$\boldsymbol{K}_E = \boldsymbol{D}\boldsymbol{K}_e\boldsymbol{B} \tag{9}$$

where $\boldsymbol{K}_e$ is the element stiffness matrix, and $\boldsymbol{B} = \boldsymbol{D}^T$ is the compatibility matrix between the member elongation and nodal displacements. Note that the fixed degrees of freedom have been appropriately removed. Element stiffness matrix $\boldsymbol{K}_e$ is a diagonal matrix that can be written as

$$\boldsymbol{K}_e = \text{diag}\left(\frac{e^i A^i}{L^i}\right) \tag{10}$$

where e^i represents the Young's modulus of member i, and A^i is the cross-sectional area of member i computed by Eq. (5) or (6).

Geometric stiffness matrix is a block-diagonal matrix composed of the force density matrix as

$$\boldsymbol{K}_G = \begin{bmatrix} \boldsymbol{G} & & \\ & \boldsymbol{G} & \\ & & \boldsymbol{G} \end{bmatrix} \tag{11}$$

The force density matrix is derived from

$$\boldsymbol{G} = \boldsymbol{C}^T \boldsymbol{Q} \boldsymbol{C} \tag{12}$$

where $\boldsymbol{Q}$ is the diagonal matrix that has the elements of force density vector $\boldsymbol{q}$ in the diagonal terms, which are calculated by

$$\boldsymbol{q} = \left(\frac{T^1(\boldsymbol{\alpha})}{L^1}, \dots, \frac{T^m(\boldsymbol{\alpha})}{L^m} \right)^T \tag{13}$$

Hence, $\boldsymbol{K}_G$ and, accordingly, $\boldsymbol{K}_T$ is a function of $\boldsymbol{\alpha}$.

Note from Eq. (11) that the geometric matrix $\boldsymbol{K}_G$ has the same matrix $\boldsymbol{G}$ in three directions, which leads to invariance of $\boldsymbol{K}_G$ with respect to a rigid-body rotation, and accordingly, invariance with respect to the coordinate system (Zhang and Ohsaki, 2007). This means that the term T^i / L^i exists in the axial direction of member. However, the absolute values of strains of members are usually very small under initial prestress, and the geometric stiffness T^i / L^i in the axial direction is small enough compared with the elastic axial stiffness $e^i A^i / L^i$. Thus, the influence of initial prestress on axial stiffness is very small (Guest, 2006; Chen and Feng, 2012; Sultan, 2013).

Eigenvalues of the tangent stiffness matrix $K_T(\boldsymbol{\alpha})$ can be taken as properties representing stiffness in the principal directions of the structure, and larger eigenvalues lead to larger global stiffness of the structure. However, it is not possible to assign lower bound for all eigenvalues for a large-scale structure. Therefore, the minimum eigenvalue $\lambda_{\min}^K(\boldsymbol{\alpha})$ of $K_T(\boldsymbol{\alpha})$ is taken as the stiffness measure in the weakest direction of displacement, and the second objective function is $\lambda_{\min}^K(\boldsymbol{\alpha})$, which is to be maximized. Therefore, for the minimization problem, $F_2(\boldsymbol{\alpha})$ is given as

$$F_2(\boldsymbol{\alpha}) = -\lambda_{\min}^{K}(\boldsymbol{\alpha}) \tag{14}$$

2.2.3 Prestress variance of cables and struts

The number of member section types is an important factor that influences the complexity and cost of construction. Hence, the unevenness of prestress values of members, which is measured by its variance, is to be minimized. Struts connected to the same ring of hoop cables are usually assigned with the same sectional type in practical cable dome projects, and the number of rings is usually not more than four (e.g. the Georgia Dome and the Suncoast Dome have three and four, respectively). It is acceptable to build a large roof with three or four types of struts. Moreover, the sectional type of a compressed member is not decided only by the internal force; its length and sectional shape also need to be considered. Therefore, only the prestress variation of cables are to be optimized. Let $T_c^{\text{ave}}(\boldsymbol{\alpha})$ denote the average prestress of cables and m_c denote the number of cables, the prestress variance of cables is given as

$$D_c(\boldsymbol{\alpha}) = \sqrt{\frac{1}{m_c - 1}\sum_{i=1}^{m_c}(T_c^i(\boldsymbol{\alpha}) - T_c^{\text{ave}}(\boldsymbol{\alpha}))^2} \tag{15}$$

Therefore, the third objective function is given as

$$F_3(\boldsymbol{\alpha}) = D_c(\boldsymbol{\alpha}) \tag{16}$$

2.2.4 Maximum prestress error

The error of cable length is inevitable in the manufacturing process. Prestress, stiffness and other structural properties are affected by the cable length error. Deng *et al*. (2016) derived the relationship between cable length error and prestress error that is represented by a sensitivity matrix ***S***. The magnitude of sensitivity to cable length error can be defined by the L_2 norm of $\boldsymbol{S}$. The derivation of sensitivity matrix $\boldsymbol{S}$ can be briefly recalled as follows; see textbooks, e.g., Ohsaki (2010) for details.

Equilibrium equation in self-equilibrium state is written as

$$\boldsymbol{DT} = \boldsymbol{0} \tag{17}$$

Let $\Delta\boldsymbol{T}$ and $\boldsymbol{d}$ denote the prestress error and nodal displacement vector corresponding to the vector of member length error $\boldsymbol{\varepsilon}$. By taking variation of Eq. (17), we obtain

$$\boldsymbol{K}_G\boldsymbol{d} + \boldsymbol{D}\Delta\boldsymbol{T} = \boldsymbol{0} \tag{18}$$

The relation between the vector of net elongation $\Delta\boldsymbol{l}$ of members and nodal displacement $\boldsymbol{d}$ is expressed using the compatibility matrix $\boldsymbol{B}$ as:

$$\Delta\boldsymbol{l} + \boldsymbol{\varepsilon} = \boldsymbol{Bd} \tag{19}$$

The prestress error $\Delta\boldsymbol{T}$ is calculated as

$$\Delta\boldsymbol{T} = \boldsymbol{K}_e\Delta\boldsymbol{l} = \boldsymbol{K}_e\boldsymbol{Bd} - \boldsymbol{K}_e\boldsymbol{\varepsilon} \tag{20}$$

Incorporating Eq. (20) into (18), we obtain the following equation:

$$\boldsymbol{K}_G\boldsymbol{d} + \boldsymbol{DK}_e\boldsymbol{Bd} - \boldsymbol{DK}_e\boldsymbol{\varepsilon} = \boldsymbol{0} \tag{21}$$

which is rewritten as

$$\boldsymbol{K}_T\boldsymbol{d} - \boldsymbol{DK}_e\boldsymbol{\varepsilon} = \boldsymbol{0} \tag{22}$$

From Eq. (20), Eq. (22) and $\boldsymbol{D} = \boldsymbol{B}^T$, we obtain

$$\Delta\boldsymbol{T} = \boldsymbol{K}_e(\boldsymbol{BK}_T^{-1}\boldsymbol{B}^T\boldsymbol{K}_e - \boldsymbol{I})\boldsymbol{\varepsilon} \tag{23}$$

from which the sensitivity matrix can be defined as

$$\boldsymbol{S} = \boldsymbol{K}_e(\boldsymbol{BK}_T^{-1}\boldsymbol{B}^T\boldsymbol{K}_e - \boldsymbol{I}) \tag{24}$$

According to Eq. (24), the error sensitivity matrix is symmetric; therefore we obtain

$$\boldsymbol{S}^T = \boldsymbol{S}, \quad \boldsymbol{S}^2 = \boldsymbol{S}^T\boldsymbol{S} \tag{25}$$

Then, the maximum eigenvalue $\lambda_{\max}^{s}$ of $\boldsymbol{S}^2$ is obtained to represent the maximum prestress error against the length error vector $\boldsymbol{\varepsilon}$ of the same norm. The fourth objective function is express as

$$F_4(\boldsymbol{\alpha}) = \lambda_{\max}^{s} \tag{26}$$

2.3 Constraints and optimization method

In a cable-strut structure, cables are supposed to be tensioned and struts are to be compressed. Therefore, the prestress values should be positive for cables and negative for struts. Moreover, members of cable-strut structures should not be slack under any load case. Thus, the absolute prestress values of members should not be too small. Accordingly, the constraints are assigned as:

$$\begin{cases} T_c^i \geq \overline{T} & \text{for } (i = 1, \dots, m_c) \\ T_s^i \leq -\overline{T} & \text{for } (i = 1, \dots, m_s) \end{cases} \tag{27}$$

where $\overline{T}$ is an appropriate positive value. In the numerical examples, Pareto optimal solutions are found using the NSGA-II, which is one of the commonly used methods for multi-objective structural optimization problems. The value of $\overline{T}$ is 1000 N, and the individuals that are incompatible with Eq. (27) are eliminated from the population.

3 Multiple criteria selection

The Pareto front of the multi-objective optimization problem described in Section 2 consists of a number of solutions that satisfy the constraints in Eq. (27). However, only one of them is to be utilized in practical design. The challenge is how to select the “most preferred solution" or how to rank the Pareto solutions.

The most preferred solution is selected through *a posteriori* process called Multi-Criteria Decision Making (MCDM). In the past few decades various MCDM methods have been proposed, among which PROMETHEE II (Brans *et al*., 1986) is one of the most effective and stable method. Since the MCDM is the post-process to the multi-objective optimization, the objective functions of Pareto optimal solutions are selected as the criteria of PROMETHEE II.

In PROMETHEE II, one alternative is compared with others based on each criterion to obtain the *preference flow*. Let a_1, $a_2, \ldots, a_n$ denote the n Pareto solutions obtained from the optimization process, and c_1, c_2, …, c_m denote m criteria. The four objective values are taken as the criteria here to evaluate the Pareto solutions. The preference flow (net flow) is the sum of *leaving flow* $f^+(a_i)$ and *entering flow* $f^-(a_i)$ as

$$f(a_i) = f^+(a_i) - f^-(a_i) \tag{28}$$

where the leaving flow and entering flow are first calculated using *preference index* $\Pi(a_i, a_j)$ as

$$f^+(a_i) = \sum_{j=1}^{n} \Pi(a_i, a_j) \tag{29}$$

$$f^-(a_i) = \sum_{j=1}^{n} \Pi(a_j, a_i) \tag{30}$$

From Eqs. (29) and (30), $f^+(a_i)$ and $f^-(a_i)$ represent the sum of $\Pi(a_i, a_j)$ and $\Pi(a_j, a_i)$, respectively, of solution a_i over all other solutions. The preference index $\Pi(a_j, a_i)$ is defined as the weighted sum of *preference function* $P_k(a_i, a_j)$, which shows the preference relationship of a_i over a_j based the kth criterion; i.e., $\Pi(a_i, a_j)$ is expressed as follows using the weight factor ω_k for the *k*th criterion:

$$\Pi(a_i, a_j) = \frac{\sum_{k=1}^{m} \omega_k P_k(a_i, a_j)}{\sum_{k=1}^{m} \omega_k} \tag{31}$$

To describe the preference relationship between solutions, Brans *et al*. (1986) presented six types of preference functions. In this paper, two of them, which are Usual Preference (UP) and Linear Preference (LP), are selected to conduct the ranking process. In the UP, $P_k(a_i, a_j) = 1$ if a_i is more preferred than a_j in view of the *k*th criterion; otherwise, $P_k(a_i, a_j) = 0$; i.e., the preference function of UP is expressed as

$$P_k(a_i, a_j) = \begin{cases} 0 & c_k(a_i) \le c_k(a_j) \\ 1 & c_k(a_i) > c_k(a_j) \end{cases} \tag{32}$$

UP is a simple and effective function to determine the preference order in a pair of solutions. However, UP simply expresses whether a solution is preferred or not over another solution, and the extent of preference is neglected. When the numbers of solutions and criteria increase, the probability of different solutions have the same value of preference flow will also increase, because there are only two preference function values, i.e., 0 and 1, in UP. Thus, LP will be adopted when the numbers of solutions and criteria are large. LP expresses the preference and its extent at the same time, and the extent is represented by the ratio of difference between the values of $c_k(a_i)$ of two solutions to the range of $c_k(a_i)$ among all solutions. The preference function of LP is defined as

$$P_k(a_i, a_j) = \begin{cases} 0 & c_k(a_i) \le c_k(a_j) \\ (c_k(a_i) - c_k(a_j)) / (c_k^{\max} - c_k^{\min}) & c_k(a_i) > c_k(a_j) \end{cases} \tag{33}$$

4 Examples

4.1 Kiewitt form cable dome

An optimization result of Kiewitt form cable dome with a diameter 60 m is presented to verify the proposed multi-objective optimization method. The dome has two rings of hoop cables, whose diameters are 20 and 40 m, respectively. Using symmetry conditions, the dome is divided into 12 equal parts. Figures 1 and 2 show the top and perspective views of the Kiewitt dome, respectively, and the member numbers are shown in Fig. 3 for one of the 12 equal parts.

The strength reduction coefficient η is 0.25. As the previous studies showed, the buckling of strut may occur when prestress increases and the structural stiffness will also be reduced (Ashwear and Eriksson,2014; Ashwear et al., 2016). Therefore, in this study, the strength reduction factor φ is introduced in Eq.(6). According to Chinese Standard for Design of Steel Structures (Ministry of Housing and Urban-Rural Development of China, 2017), the slenderness ratio of compressed members, which is the ratio of effective length to radius of gyration, is restricted to not more than 150. Here, the slenderness ratios of all the strut are assumed to be 150; accordingly, the stability reduction coefficient φ is 0.339. Since the slenderness are restricted to be less than 150, we do not have to consider member buckling of struts owing to the small value of φ.

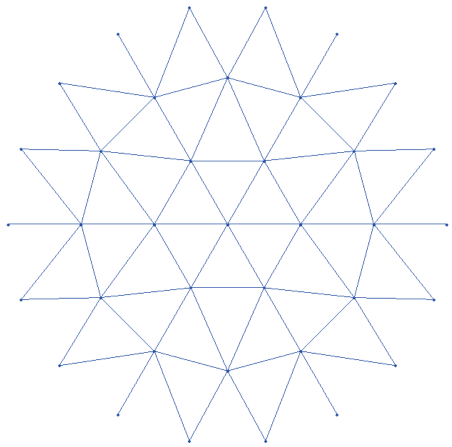

Fig.1 Top view

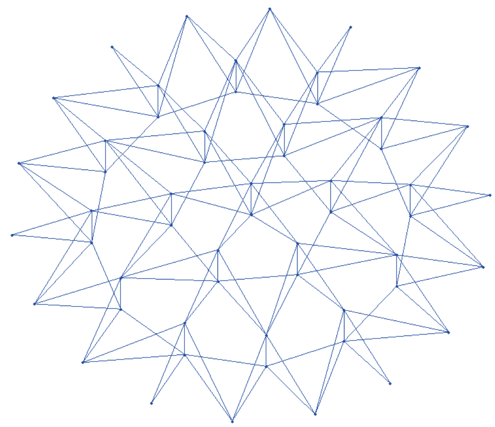

Fig.2 Perspective view

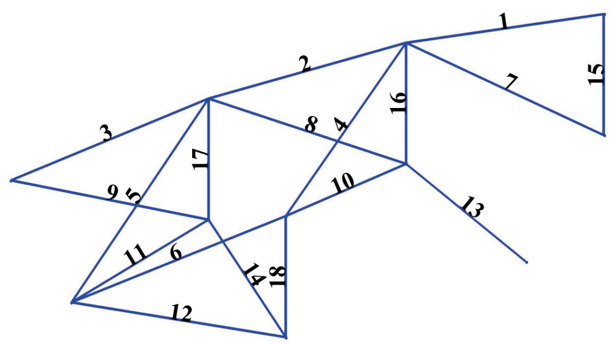

Fig.3 Element numbers

There are four self-stress modes, as shown in Table 1, considering symmetry conditions. Here, the “self-stress modes considering symmetry” can also be written as “integral self-stress states” or “self-stress states with full symmetry” (Yuan *et al*, 2007; Chen *et al*, 2018b). The self-stress modes listed in Table 1 is one possible basis for the null space of the equilibrium matrix. Different self-stress modes may be obtained, since linear combinations of self-stress modes in Table 1 can also be a basis for the null space of the equilibrium matrix. The parameters of NSGA-II for this example are listed in Table 2. We confirmed that similar solutions are obtained from several different initial solutions, and all solutions converge to Pareto optimal solutions.

Table 1 Self-stress modes of Kiewitt dome

Member No.	Self-stress mode No.			
	1	2	3	4
1	0.00537	0.1032	-0.02727	0.00129
2	0.13391	-0.05343	-0.01827	0.00163
3	-0.15171	0.18287	0.01012	-0.00042
4	-0.02416	0.07584	0.14128	-0.12822
5	-0.06294	0.09113	-0.21793	0.16055
6	0.12782	-0.02037	0.01434	0.00203
7	0.13804	0.1728	0.00423	0.00525
8	-0.02837	-0.03562	0.01171	0.01473
9	0.04655	0.05695	0.15806	0.1987
10	0.04028	0.0326	-0.02191	0.00101
11	-0.01633	-0.02412	0.00995	-0.00055
12	0.06943	-0.0084	-0.03145	0.00087
13	-0.00271	-0.0522	0.0138	-0.00065
14	0.00082	0.0158	-0.00418	0.0002
15	-0.02731	-0.03419	-0.00084	-0.00104
16	0.02391	0.03099	-0.12622	-0.1587
17	0.04342	0.05435	0.00133	0.00165
18	-0.02003	0.03711	0.00568	0.00021

Note: the self-stress modes in this table is only one possible basis for the null space of the equilibrium matrix, different self-stress modes may be obtained.

Table 2 Parameters for optimization of Kiewitt dome

Parameter	value
Population size	200
Number of Generations	1000
Crossover probability	0.5
Mutation probability	0.25
Crossover distribution index	20
Mutation distribution index	100

The Pareto optimal solutions are plotted in Fig. 4 in the space of F_1, F_2 and F_3. The size of each point is proportional to the value of F_4. In practical design process, only one set of prestresses is to be applied from the Pareto optimal solutions that provide the alternatives for designers to select. The PROMETHEE II is applied here to rank the solutions with weight coefficient $\omega_k = 1$ for all four criteria. The value of preference flow obtained from Eq. (28) with LP for each solution is represented by the color in Fig. 4. The red point indicates the best solution ranked by PROMETHEE-II.

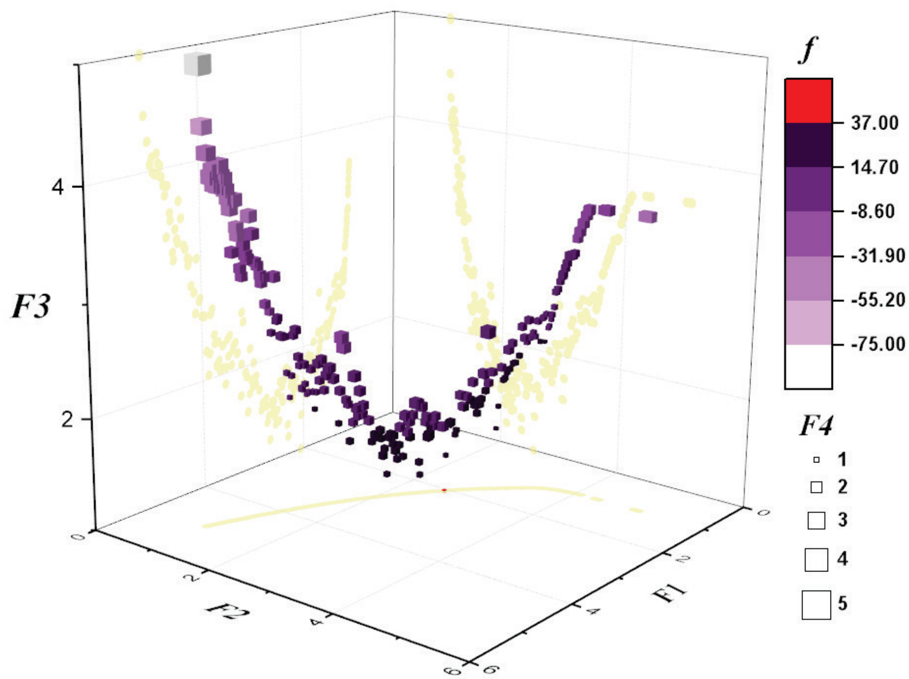

Fig. 4 Pareto front of Kiewitt dome

Yuan *et al*. (2007) and Chen *et al*. (2015) optimized the prestress of this structure with single objective function. Their solutions are compared and ranked together with the solutions obtained by the method proposed in this paper. Prestress value of cables in the outmost hoop was minimized by Yuan *et al*. (2007), while the total strain energy was minimized by Chen *et al*. (2015).

Table 3 shows the preference flow and solution numbers of top 10 solutions ranked by UP and LP. The column named ‘Compared’ represents the preference flow value taking results of Yuan *et al*. (2007) and Chen *et al*. (2015) into consideration. The ‘Pareto only’ column is the preference flow value considering the Pareto solutions of this paper only. Obviously, the ranks of UP almost remain unchanged, while the ranks of LP are significantly influenced by incorporation of the solutions by Yuan *et al*. (2007) and Chen *et al*. (2015). According to Eq. (33), the distinction of preference function between solutions will be smaller, if LP is used and an objective function value that is far from the others is considered. The result of Chen *et al*. (2015) has a reasonable value of F_2 but has considerably large values in the remaining three objective functions as shown in Fig. 5, which is the reason for the rank deviation when LP is used.

As shown in Table 3, solution No.79 is the first place solution via UP and LP in both cases. Therefore solution No.79 might be taken as 'the best' solution among all the solutions and is recommended for practical design.

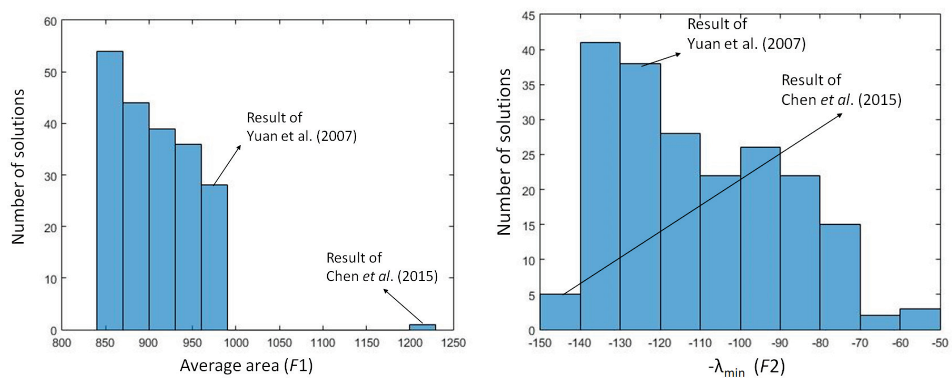

(a) distribution of average area (b) distribution of $-\lambda_{min}$

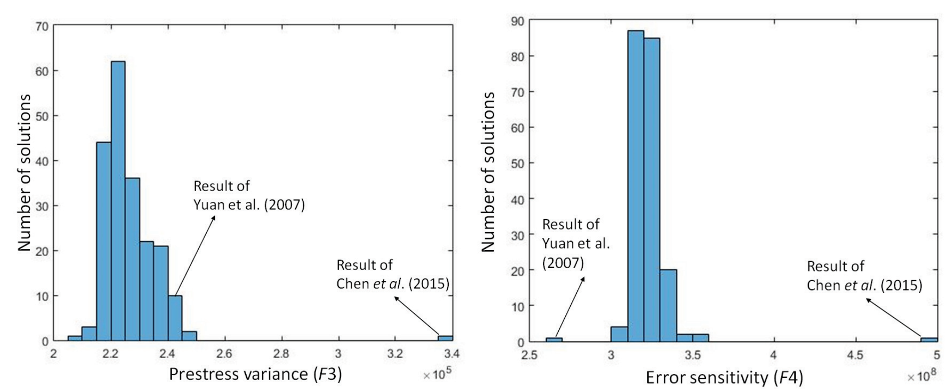

(c) distribution of prestress variance (d) distribution of error sensitivity

Fig. 5 Distribution of 'Compared' solutions of Kiewitt dome

For all the 200 solutions, there are only 158 different values of preference flow value via UP, which means the ranks of solutions may not be uniquely determined. Meanwhile, duplicate preference flow value did not occur via LP. However, the ranking results of the LP is significantly influenced by the distribution of solutions. It is recommended to check the distribution of solutions and filter the solutions according to structural demands before using the LP.

In Table 4, the value of objective functions and combination coefficients are shown. Compared with multi-objective solutions, the single-objective solutions of Yuan *et al.*(2007) and Chen *et al.* (2015) are not ranked to the top according to the four objects of this paper. Their results both take advantage of stiffness to some extent, but fall behind in other measures. However, if the emphasis of the structural requirement is on stiffness their results are better than the 10 highest ranking Pareto solutions.

Table 3 Ranking of Pareto solutions of Kiewitt dome

Rank	Linear Preference (LP)				Rank	Usual Preference(UP)			
	Compared		Pareto only			Compared		Pareto only	
	f	Sol. No.	f	Sol. No.		f	Sol. No.	f	Sol. No.
1	99.00	79	98.5	79	1	10.64	79	37.63	79
2	93.00	78	92.5	78	2	10.31	78	31.62	53
3	91.50	90	91	90	3	9.73	90	31.29	54
4	88.00	53	87.5	53	4	9.55	53	28.82	78
5	87.00	54	86.5	54	5	9.35	54	28.71	90
6	83.00	108	82.5	108	6	9.34	108	25.57	108
7	76.00	75	75.5	75	7	9.25	75	24.96	52
8	73.00	52	72.5	52	8	9.20	52	23.52	75
9	73.00	99	72.5	99	9	9.16	99	23.02	91
10	72.00	109	71.5	109	10	8.97	109	22.62	74
140	-18.00	Yuan	-	-	42	6.77	Yuan	-	-
202	-100.50	Chen	-	-	202	-110.10	Chen	-	-

Note: f is the preference flow value according to Eq. (28).

Table 4 Detailed results of Pareto solutions of Kiewitt dome

rank	Avg. area (mm^2)	$-\lambda_{min}$	Prestress variance (N)	Max. error norm	Combination coefficient			
					α_1	α_2	α_3	α_4
1	945.2	-130.6	2.22×10^5	3.10×10^8	2.683	4.666	-1.620	0.268
2	934.9	-127.2	2.21×10^5	3.11×10^8	2.791	4.675	-1.548	0.473
3	938.0	-128.4	2.23×10^5	3.13×10^8	2.785	4.783	-1.615	0.434
4	937.2	-128.1	2.23×10^5	3.13×10^8	2.804	4.796	-1.622	0.459
5	938.8	-128.5	2.23×10^5	3.13×10^8	2.810	4.810	-1.664	0.444
6	944.2	-130.4	2.24×10^5	3.14×10^8	2.653	4.659	-1.642	0.321
7	940.0	-129.0	2.23×10^5	3.15×10^8	2.733	4.856	-1.614	0.386
8	940.2	-129.0	2.23×10^5	3.15×10^8	2.732	4.857	-1.618	0.385
9	935.6	-127.6	2.23×10^5	3.14×10^8	2.824	4.870	-1.613	0.492
10	946.3	-131.0	2.25×10^5	3.15×10^8	3.214	5.829	-2.017	0.327
Yuan	1014.6	-128.8	2.08×10^5	2.62×10^8	2.377	3.202	-0.972	-0.397
Chen	1267.0	-141.6	3.40×10^5	4.91×10^8	2.393	3.219	-0.901	-0.312

4.2 Spatial Cable-truss

The spatial cable-truss is on a circular boundary with a diameter of 72 m. There are 12 radial branches and three rings of hoops. All the members are classified into nine groups. The detailed configuration is shown in Figs. 6 and 7. There are three self-stress modes as shown in Table 5 (Zhang and Feng, 2017). The strength reduction coefficients η and φ are 0.25 and 0.339, respectively.

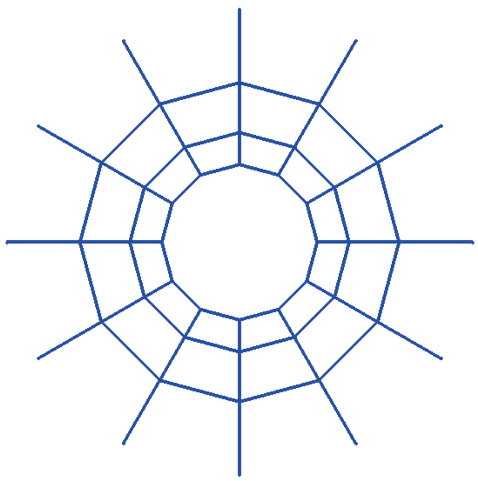

Fig.6 Top view of spatial cable-truss

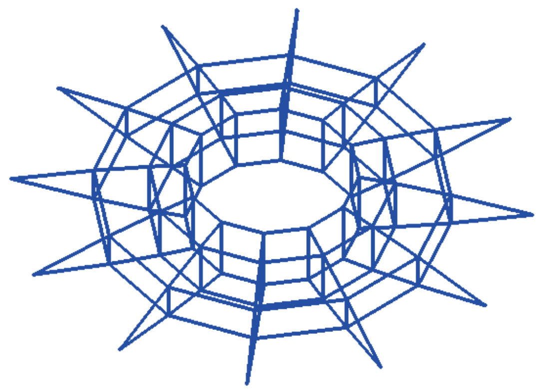

Fig.7 Perspective view of spatial cable-truss

The parameters of this example for NSGA-II are listed in Table 6. The obtained Pareto solutions are plotted in Fig. 8. Similarly to the previous example, the three axes are F_1, F_2 and F_3, respectively, and the size of plotted cubes represent the value of F_4. The preference flow obtained by LP is represented by the color of cubes. The best solution is marked red.

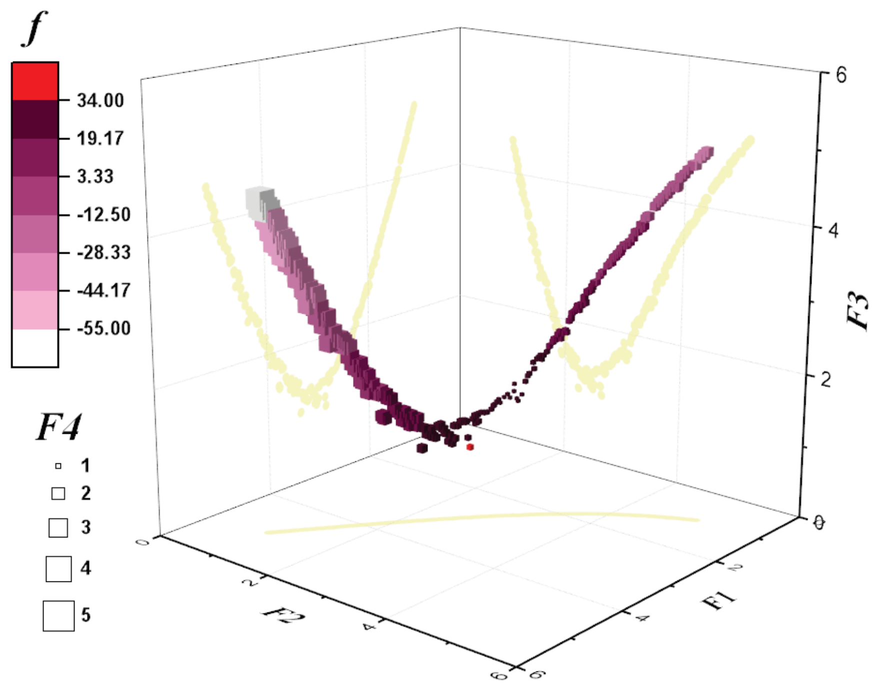

Fig. 8 Pareto front of spatial cable-truss

Table 5 Self-stress modes of spatial cable-truss

Member No.	Self-stress mode No.		
	1	2	3
1	-0.0420	0.0663	-0.0987
2	-0.0536	0.0896	-0.004
3	-0.0842	0.0029	-0.0003
4	0.0227	0.0453	-0.1778
5	0.0592	0.1644	-0.007
6	-0.1608	0.0055	-0.0005
7	-0.0004	0.0015	0.0225
8	-0.0024	0.0167	0.0007
9	0.0126	-0.0004	0

Note: the self-stress modes in this table is only one possible basis for the nullspace of the equilibrium matrix, different self-stress modes may be obtained.

Table 6 Parameters for optimization of cable truss

Parameter	Value
population size	200
Number of Generations	1000
Crossover probability	0.5
Mutation probability	0.33
Crossover distribution index	20
Mutation distribution index	100

To select the most preferred self-stress combination among Pareto solutions, the PROMETHEE-II is adopted with weight coefficients of all criteria to be 1. Zhang and Feng (2017) obtained three kinds of solutions by optimizing the prestress of this structure to maximize the minimum eigenvalue of geometric stiffness matrix, which is similar to our function in F_2 which is the minimum eigenvalue of tangential stiffness matrix including the effect of linear stiffness. Meanwhile, Zhang and Feng incorporated unilateral conditions of members and unevenness of prestress as constraints. The solutions of NSGA-II and results of Zhang and Feng are compared and ranked together by UP and LP, as listed in Table 7

Table 7 Ranking of Pareto solutions of cable-truss

Rank	Linear Preference (LP)				Rank	Usual Preference (UP)			
	Compared		Pareto only			Compared		Pareto only	
	f	Sol. No.	f	Sol. No.		f	Sol. No.	f	Sol. No.
1	81.50	107	81.00	107	1	30.15	107	34.70	107
2	74.00	90	73.50	108	2	28.88	90	32.20	108
3	74.00	89	73.00	90	3	28.59	89	32.19	90
4	72.50	87	72.00	102	4	28.33	87	31.75	89
5	72.00	92	71.50	104	5	28.21	92	31.68	83
6	71.50	83	70.50	83	6	28.14	83	31.61	87
7	71.50	96	70.50	89	7	28.14	96	31.57	96
8	71.50	108	70.50	98	8	28.03	108	31.48	92
9	71.00	94	70.00	87	9	27.99	94	31.31	95
10	71.00	95	70.00	97	10	27.98	95	31.31	84
99	4.00	Zhang(1)	-	-	131	-7.43	Zhang(1)	-	-
66	38.50	Zhang(2)	-	-	36	23.64	Zhang(2)	-	-
92	8.00	Zhang(3)			105	2.39	Zhang(3)		

Note: f is the preference flow value according to Eq. (28)

Zhang(1), Zhang(2) and Zhang(3) are the solutions of Zhang and Feng (2017)

Table 8 Detailed results of Pareto solutions of cable-truss

Rank	Avg. area (mm^2)	λ_{min}	Prestress variance (N)	Max. error norm	Combination coefficient		
					α_1	α_2	α_3
1	845.8	-10.28	1.75×10^5	3.73×10^8	-3.615	1.535	-4.626
2	846.2	-10.37	1.82×10^5	3.90×10^8	-3.597	1.371	-4.420
3	838.9	-9.25	2.06×10^5	2.96×10^8	-1.946	0.632	-3.061
4	838.1	-9.11	2.10×10^5	2.89×10^8	-3.903	1.223	-6.310
5	835.2	-8.57	2.07×10^5	3.00×10^8	-1.694	0.724	-3.334
6	836.8	-8.89	2.10×10^5	2.93×10^8	-3.715	1.283	-6.461
7	840.9	-9.57	2.02×10^5	3.25×10^8	-3.929	1.265	-5.701
8	839.6	-9.37	2.06×10^5	3.08×10^8	-3.134	0.978	-4.755
9	840.4	-9.50	2.04×10^5	3.20×10^8	-4.014	1.259	-5.902
10	835.5	-8.62	2.09×10^5	3.00×10^8	-3.115	1.242	-5.961
Zhang(1)	879.4	-14.59	1.85×10^5	7.13×10^8	-0.696	0.647	-0.313
Zhang(2)	862.7	-12.28	1.11×10^5	4.46×10^8	-0.587	0.605	-0.538
Zhang(3)	824.0	-5.29	2.47×10^5	3.57×10^8	-0.097	0.297	-0.950

The top solutions selected by UP and LP are all from the solutions of this paper; none of the solutions of Zhang and Feng (2017) ranked into the top 10%. The 'Compared' rank and 'Pareto only' are the same for this example because the results of Zhang and Feng (2017) are distributed inside the solutions of this paper as seen in Fig. 9. The best one of LP and UP are both No.107.

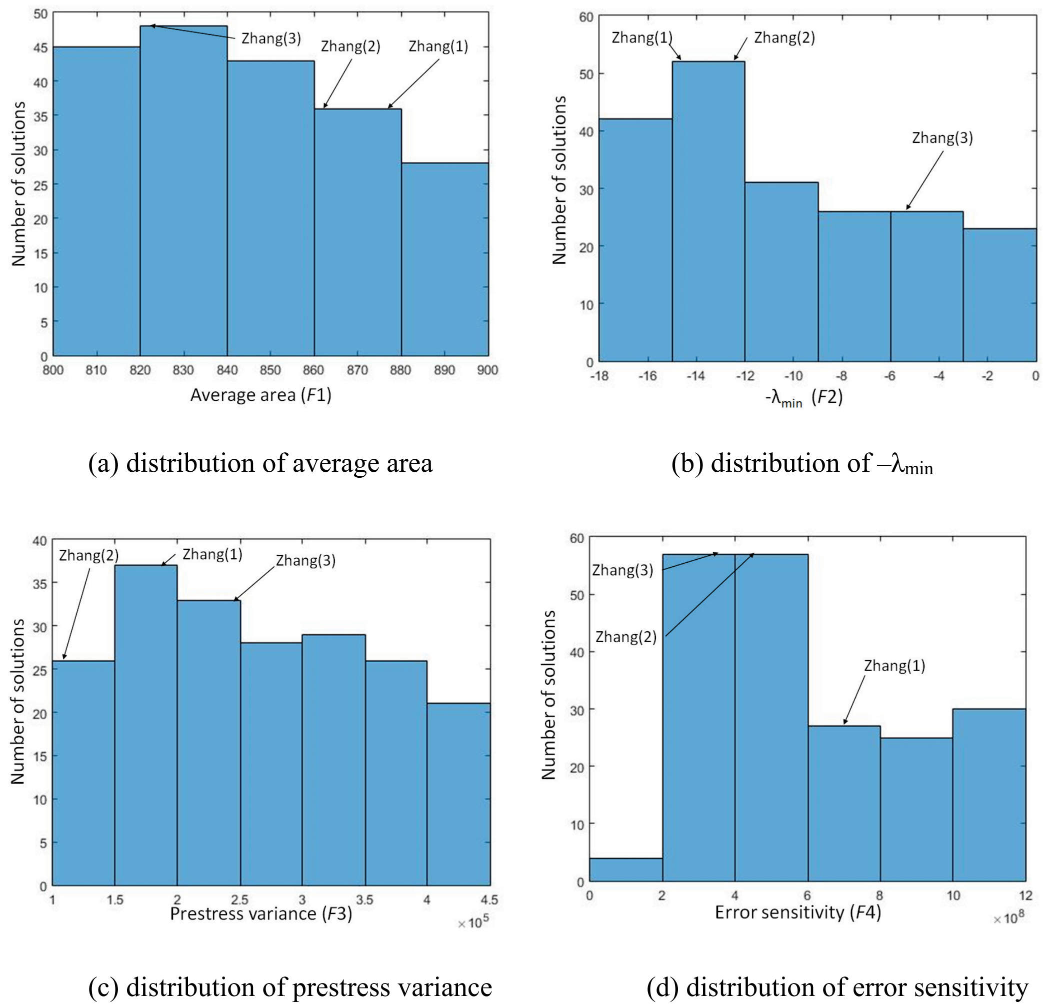

(a) distribution of average area

(b) distribution of $-\lambda_{min}$

(c) distribution of prestress variance

(d) distribution of error sensitivity

Fig. 9 Distribution of 'Compared' solutions of spatial cable-truss

The rank of the solutions of Zhang and Feng are relatively low both by UP and LP. Therefore, for problem considering multiple requirement, the solutions of multi-objective optimization are more stable and robust, i.e., it is more likely to obtain more preferred solutions by optimizing the prestress with multiple objectives simultaneously than with single objective separately.

4.3 Significance of each objective function

In order to evaluate the significance of each objective function, the number of Pareto solutions is calculated after removing each objective function. Note that the Pareto set is fixed at the set obtained by considering the four objective functions. The objective function is regarded as insignificant if the number of Pareto solutions remains almost the same after removing the objective function.

Table 9 Number of Pareto solutions and rank deviation after removing each objective function

		removed objective function			
	model	F_1	F_2	F_3	F_4
No. of remained Pareto solutions	Kiewitt	61	105	199	99
	Cable-truss	96	86	200	198
Avg. rank deviation	Kiewitt	41.44	29.30	22.48	18.03
	Cable-truss	27.33	22.74	30.86	27.28

If the remained solutions are considered, it is seen from Table 9 that the most influential objective function for both of the two models is the average cross-sectional area F_1. The prestress variance F_3 has little influence on both two models. However, the importance of maximum prestress error F_4 to the two models are different. The eigenvalue F_2 representing stiffness is more influential for spatial cable-truss than for Kiewitt dome.

However, if the average rank deviation is considered, as shown in Table 9, the most influential objective function on the remained number of solutions may not play the same role on the rank deviation. For the cable-truss, F_4 impacts the rank almost the same as F_1, while it makes large difference in remaining Pareto solution number. However, for the Kiewitt dome, the most and least influential objective function on rank is F_1, which is the same as the function on the remaining number of Pareto solutions.

Therefore, different results of the significant objective functions are obtained when different criteria and structures are applied. Even the least influential objective functions judged by one criterion should not be neglected. In practical design, importance of objective functions should be selected based on comprehensive consideration of each design objective.

5 Conclusion

Structural behavior of cable-strut structures significantly depends on the values and distribution of prestress. In this paper, the coefficients of self-equilibrium prestresses of cable-strut structures are optimized for four objective functions that represent the material cost, stiffness, types of member sections and insensitivity to cable length error. Pareto solutions with respect to the four objective functions are obtained by NSGA-II. The method of multiple criteria decision analysis called PROMETHEE-II is adapted to rank the solutions and find the most preferred solution. The conclusions are summarized as follows:

(1) Multi-objective optimization is capable of obtaining prestress that meets various structural demands. By solving a multi-objective optimization problem, a higher possibility to obtain solutions with higher preference can be obtained than solving a single-objective optimization problem.

(2) The most preferred solution can be found by filtering Pareto solutions using

PROMETHEE-II. Usual Preference is more stable with respect to the distribution of solution values but may have the problem of duplicate rank. Linear Preference gives a unique score to each solution; however, it may be significantly influenced by solution values. Comprehensive comparison and consideration are recommended to select the most preferred solution.

(3) Evaluate the impact of each objective function is important after solving a problem with several objective functions, because unnecessary functions may be removed for the practical design process. For this purpose, the number and rank deviation of Pareto solutions after removing an objective function may be useful measures of the significance of the objective function.

6 Acknowledgement

This work is sponsored by the National Natural Science Foundation of China (Grant No. 51478310) and the Science and Technology Program of Ministry of Housing and Urban-Rural Development of China (No. 2016-K5-062). The authors also appreciate the support provided by the Chinese Scholarship Council (File No. 201706250070) that enabled the author to conduct research with Prof. M. Ohsaki at Kyoto University.

7 Reference

Adam, B., Smith Ian, F. (2007). Tensegrity active control: Multiobjective approach. Journal of Computing in Civil Engineering, 21(1), 3-10.

Ashwear, N., Tamadapu, G., Eriksson, A. (2016). Optimization of modular tensegrity structures for high stiffness and frequency separation requirements. International Journal of Solids and Structures, 80, 297-309.

Ashwear, N., Eriksson, A. (2014). Natural frequencies describe the pre-stress in tensegrity structures. Computers & Structures 138: 162-171.

Branke, J., Branke, J., Deb, K., Miettinen, K., Slowiński, R. (Eds.). (2008). Multiobjective optimization: Interactive and evolutionary approaches (Vol. 5252). Springer Science and Business Media.

Brans, J.-P., Vincke, P., Mareschal, B. (1986). How to select and how to rank projects: The PROMETHEE method. European Journal of Operational Research, 24(2), 228-238.

Brochoff, D., Saxena, D. K., Deb, K., and Zitzler, E. (2008). On handling a large number of objectives a posteriori and during optimization. In: Multiobjective Problem Solving from Nature, Knowles, J., Corne, D., Deb., K. (eds.), pp. 377-403, Springer.

Chen, L., Zhou, Y., Dong, S. (2015). Overall self-stress modes analysis and optimal prestress design of the Kiewitt Dome. Journal of the International Association for Shell and Spatial Structures, 56(2), 113-123.

Chen, Y. and Feng, J. (2012). Generalized eigenvalue analysis of symmetric prestressed structures using group theory. Journal of Computing in Civil Engineering 26(4): 488-497.

Chen, Y., Feng, J. and Wu, Y. (2012). Novel form-finding of tensegrity structures using ant colony systems. 4(3): 031001.

Chen, Y., Sun Q. and Feng, J. (2018a). Stiffness degradation of prestressed cable-strut structures observed from variations of lower frequencies. Acta Mechanica: 1-14.

Chen, Y., Feng, J., Lv, H. and Sun, Q. (2018b). Symmetry representations and elastic redundancy for members of tensegrity structures. 203: 672-680.

Deb, K., Pratap, A., Agarwal, S., and Meyarivan, T. A. M. T. (2002). A fast and elitist multiobjective genetic algorithm: NSGA-II. IEEE transactions on evolutionary computation, 6(2), 182-197.

Deng, H., Zhang, M., Liu, H., Dong, S., Zhang, Z., Chen, L. (2016). Numerical analysis of the pretension deviations of a novel crescent-shaped tensile canopy structural system. Engineering Structures 119: 24-33.

Emmerich, D. G. (1996). Emmerich on self-tensioning structures. International Journal of Space Structures, 11(1-2), 29-36.

Figueira, J., Greco, S., Ehrogott, M. (2005). Multiple Criteria Decision Analysis: State of the Art Surveys. Springer New York.

Fuller, R. B., & Applewhite, E. J. (1975). Synergetics: Explorations in the Geometry of Thinking. Macmillan Pub. Co.

Gal, T., Leberling, H. (1977). Redundant objective function in linear vector maximum problems and their determination. European Journal of Operational Research, 1, 176-184.

Geiger, D. H., Stefaniuk, A., Chen, D. (1986). The design and construction of two cable domes for the Korean Olympics. Proceedings of Symposium of International Association for Shell and Spatial Structures (IASS1986), 265–272.

Guest, S.D., 2006. The stiffness of prestressed frameworks: a unifying approach. International Journal of Solids and Structures 43, 842–854.

Lee, S., Lee, J. (2014). Optimum self-stress design of cable–strut structures using frequency constraints. International Journal of Mechanical Sciences, 89, 462–469.

Levy, M. P. (1994). The Georgia Dome and beyond: Achieving lightweight-longspan structures. In: Spatial, Lattice and Tension Structures, IASS-ASCE International Symposium, 560–562.

Ministry of Housing and Urban-Rural Development of China (2017). Standard for design of steel structures (GB50017-2017).

Motro, R. (2003). Tensegrity: Structural Systems for the Future. Elsevier.

Ohsaki, M. (2010). Optimization of Finite Dimensional Structures, CRC Press, 2010.

Ohsaki, M., Zhang, J., Elishakoff, I. (2012). Multiobjective hybrid optimization-antioptimization for force design of tensegrity structures. Journal of Applied Mechanics, 79(2), 021015.

Ohsaki, M., Zhang, J., Ohishi, Y. (2008). Force design of tensegrity structures by enumeration of vertices of feasible region. International Journal of Space Structures, 23(2), 117-125.

Pellegrino, S., Calladine, C. R. (1986). Matrix analysis of statically and kinematically indeterminate frameworks. International Journal of Solids and Structures, 22(4), 409-428.

Safaei, S. D., Eriksson, A., Tibert, G. (2012). Optimum pre-stress design for frequency requirement of tensegrity structures. Proceedings of 10th World Congress in Computational Mechanics (WCCM10), Sao Paulo, Brazil.

Schek, H. J. (1974). The force density method for form finding and computation of general networks. Computer Methods in Applied Mechanics and Engineering 3(1): 115-134.

Snelson, K. (1996). Snelson on the tensegrity invention. International Journal of Space Structures, 11(1-2), 43-48.

Sultan, C. (2013). Stiffness formulations and necessary and sufficient conditions for exponential stability of prestressable structures. International Journal of Solids and Structures 50(14-15): 2180-2195.

Tusar, T., Filipic, B. (2015). Visualization of pareto front approximations in evolutionary multiobjective optimization: A critical review and the prosection method. Evolutionary Computation IEEE Transactions on, 19(2), 225-245.

Xu, X., Luo, Y. (2008). Multi-objective shape control of prestressed structures with genetic algorithms. Proceedings of the Institution of Mechanical Engineers, Part G: Journal of Aerospace Engineering,

Yuan, X., Chen, L., Dong, S. (2007). Prestress design of cable domes with new forms. International Journal of Solids and Structures, 44(9), 2773-2782.

Zhang, J.Y., Guest, S.D., Ohsaki, M. (2009). Symmetric prismatic tensegrity structures: Part I. Configuration and stability. International Journal of Solids and Structures 46(1): 1-14.

Zhang, J.Y., Ohsaki M. (2015). Tensegrity structures: form, stability, and symmetry. Mathematics for Industry Series, Springer.

Zhang J. Y., Ohsaki, M. (2007). Stability conditions for tensegrity structures. International Journal of Solids Structures 44(11-12): 3875-3886.

Zhang, P., Feng, J. (2017). Initial prestress design and optimization of tensegrity systems based on symmetry and stiffness. International Journal of Solids and Structures, 106-107, 68-90.